Progress In Electromagnetics Research M, Vol. 17, 101–111, 2011

EFFICIENT SIMULATIONS OF PERIODIC STRUCTURES WITH OBLIQUE INCIDENCE USING DIRECT SPECTRAL FDTD METHOD

Y. J. Zhou, X. Y. Zhou, and T. J. Cui

Institute of Target Characteristics and Identification
State Key Laboratory of Millimeter Waves, School of Information Science and Engineering, Southeast University
Nanjing, Jiangsu 210096, China

R. Qiang and J. Chen

Department of Electrical and Computer Engineering
University of Houston, Houston, TX 77204-4005, USA

Abstract—A simple and efficient joint algorithm of finite difference time domain (FDTD) and periodic boundary condition (PBC), called as the direct spectral FDTD method, has been investigated to study three-dimensional (3D) periodic structures with oblique incidence, where both the azimuth angle ϕ and the elevation angle θ are varying. The number of sampling points for the horizontal wave number can be determined by using an adaptive approach. As numerical results, the transmission and reflection coefficients from split-ring resonators (SRRs) and a dielectric grating slab are computed to validate the accuracy and efficiency of the direct spectral FDTD method. The computed results are in good agreement to the published ones obtained by other methods.

1. INTRODUCTION

Periodic structures have found more and more applications, such as the frequency selective surfaces (FSS), the electromagnetic band-gap (EBG) structures, and metamaterials, etc. It is of great importance to simulate the periodic structures accurately and efficiently using numerical methods. Finite-Difference Time-Domain (FDTD) technique, combined with periodic boundary conditions

Received 25 January 2011, Accepted 21 February 2011, Scheduled 24 February 2011
Corresponding author: Tie-Jun Cui (tjcui@seu.edu.cn).

(PBCs), has been shown as an effective method for the fast full-wave characterization of these structures.

The FDTD methods proposed for periodic structures can be classified into two categories [1]: indirect field methods based on the field transformation technique [2] and direct field methods. The former includes multi-spatial grid method [3], split-field method (SFM) [4–6], spectral FDTD method [7], and exponential time differencing method (ETD) [8, 9], etc. The later includes multiple unit cell method [10], and sine-cosine method [11], etc. Compared with indirect methods, direct field methods have many advantages: they have the same stability condition and numerical error as those of the conventional FDTD method, and have simple formulations. It also has good computational efficiency when the incident elevation angle is near the grazing incident angles.

The method of FDTD computation of plane-wave scattering problems with the constant wave-number was proposed by Aminian et al. [7], which was referred to as spectral FDTD method. Then it was further improved and simplified [12–14]. The novelty of the simple and efficient FDTD/PBC algorithm is that the direct computation of E and H fields rather than the indirect calculation using auxiliary fields [13]. Here we call the algorithm direct spectral FDTD method. In this paper, direct spectral FDTD method is extended to compute the scattering of periodic structures with arbitrary obliquely incident plane waves where both the azimuth and the elevation angles vary. An effectively adaptive method is proposed to determine the horizontal wave-number sampling points. The final part of this paper is devoted to studying two kinds of three-dimensional (3D) periodic structures where both the azimuth and the elevation angles vary. One is the split-ring resonator (SRR) and the other is a dielectric grating slab

2. FORMULATIONS

2.1. Extension of Direct Spectral FDTD Method

For a two-dimensional periodic structure shown in Figure 1, with periodicity of a along the x direction and b along the y direction, the periodic boundary conditions of the electric and magnetic fields in the frequency domain are expressed as below:

$$\begin{aligned} H(x=0,y,z) &= H(x=a,y,z)\exp(jk_x a) \\ H(x,y=0,z) &= H(x,y=b,z)\exp(jk_y b) \end{aligned} \tag{1}$$

$$\begin{aligned} E(x=a,y,z) &= E(x=0,y,z)\exp(-jk_x a) \\ E(x,y=b,z) &= E(x,y=0,z)\exp(-jk_y b) \end{aligned} \tag{2}$$

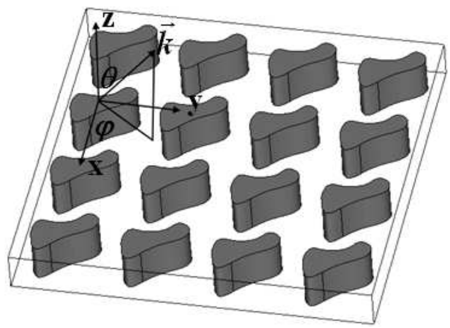

Figure 1. Sketch of two-dimensional periodic structure illuminated by a plane wave propagating along the vector $\vec{k}$ defined by Euler angles θ and φ.

where k_x and k_y are the horizontal wave numbers along the x and y direction.

The main feature of direct spectral FDTD method is to fix k_x and k_y. The periodic boundary conditions of the electric and magnetic fields in the time domain are expressed as below:

$$\begin{aligned} H(x=0,y,z,t) &= H(x=a,y,z,t)\exp(jk_x a) \\ H(x,y=0,z,t) &= H(x,y=b,z,t)\exp(jk_y b) \end{aligned} \tag{3}$$

$$\begin{aligned} E(x=a,y,z,t) &= E(x=0,y,z,t)\exp(-jk_x a) \\ E(x,y=b,z,t) &= E(x,y=0,z,t)\exp(-jk_y b) \end{aligned} \tag{4}$$

Only the incident direction $\varphi = n\pi/2$ was considered and the horizontal wave-number k_x was fixed [13]. In this paper, an arbitrary φ angle is considered. It is implemented by fixing the horizontal wave-number k_ρ, where $k_\rho = 2\pi f(\sin\theta)/C_0$ (C_0 is the light speed in free space). Hence we have

$$\begin{aligned} k_x &= k_\rho \cdot \cos\varphi_0 \\ k_y &= k_\rho \cdot \sin\varphi_0 \end{aligned} \tag{5}$$

where φ_0 is a constant parameter, and $\varphi = \varphi_0$ is the incident plane. To avoid the horizontal resonance problem, the central frequency f of the modulated Gaussian pulse is set to:

$$f = \frac{k_\rho \cdot C_0}{2\pi} + f_0 \tag{6}$$

where f_0 is the central frequency of the considered frequency band.

To calculate the space distribution of the plane wave excitation, we need to set H_x and H_y for the TM^z case and E_x and E_y for the TE^z case. The formulations are as follows:

For the TM^z case,

$$\begin{aligned} H_x^{inc}(x,y,z_0,t) = & H_x^{inc}(x,y,z_0,t) - \frac{\Delta t \cdot C_0}{\Delta} \exp\left[-\frac{(t-t_0)^2}{2\sigma_t^2}\right] \exp(j2\pi f t) \\ & \cdot \exp(-jk_x x)\exp(-jk_y y)\sin\varphi_0 \\ H_y^{inc}(x,y,z_0,t) = & H_x^{inc}(x,y,z_0,t) + \frac{\Delta t \cdot C_0}{\Delta} \exp\left[-\frac{(t-t_0)^2}{2\sigma_t^2}\right] \exp(j2\pi f t) \\ & \cdot \exp(-jk_x x)\exp(-jk_y y)\cos\varphi_0 \end{aligned} \tag{7}$$

For the TE^z case,

$$\begin{aligned} E_x^{inc}(x,y,z_0,t) = & E_x^{inc}(x,y,z_0,t) + \frac{\Delta t \cdot C_0}{\Delta} \exp\left[-\frac{(t-t_0)^2}{2\sigma_t^2}\right] \exp(j2\pi f t) \\ & \cdot \exp(-jk_x x)\exp(-jk_y y)\sin\varphi_0 \\ E_y^{inc}(x,y,z_0,t) = & E_x^{inc}(x,y,z_0,t) - \frac{\Delta t \cdot C_0}{\Delta} \exp\left[-\frac{(t-t_0)^2}{2\sigma_t^2}\right] \exp(j2\pi f t) \\ & \cdot \exp(-jk_x x)\exp(-jk_y y)\cos\varphi_0 \end{aligned} \tag{8}$$

where Δt is the time step, Δ is the diagonal length of cube-cell grid, t_0 is the time delay of the modulated Gaussian waveform, f is the central frequency, σ_t is the pulse width, t_0 is set to a value between $3\sigma_t$ to $5\sigma_t$.

2.2. Determination of the Sampling Points for k_ρ

In this section, an adaptive method is proposed to determine the number of k_ρ-sampling points. Suppose that the number of the sampling points is n. For the maximum incident angle $\theta_{\max}$ and frequency of interests $f_{\max}$, the maximum horizontal wave-number $(k_\rho)_{\max}$ is defined as

$$(k_\rho)_{\max} = \frac{2\pi f_{\max} \sin\theta_{\max}}{C_0} \tag{9}$$

and k_ρ^i, which is horizontal wave-number for each sampling point i, is given by

$$k_\rho^i = \frac{(k_\rho)_{\max}}{n} \cdot i, \quad i = 0, 1, \ldots, n-1 \tag{10}$$

Denoting $R^i(f)$ as the reflection coefficient versus frequencies corresponding to k_ρ^i, $R_{\theta_{\max}}(f)$ as the reflection coefficient versus frequencies corresponding to $\theta_{\max}$, and $R_{\theta_{\max}}^n(f)$ as the reflection coefficient versus frequencies corresponding to using n sampling points for k_ρ, the maximum relative error over the frequency range of interest is defined as

$$\epsilon = \max\left(\frac{R^{2n}_{\theta_{\max}}(f) - R^{n}_{\theta_{\max}}(f)}{R^{2n}_{\theta_{\max}}(f)}\right), \quad f = f_{\min}, \ldots, f_{\max} \tag{11}$$

The adaptive procedure is thus described as below:

1) Select an original value of n, and compute $k^i_\rho, i = 0, 1, \ldots, n-1$. For each k^i_ρ, run the simulation to obtain $R^i(f)$. After the whole n-step simulations, calculate $R^n_{\theta_{\max}}(f)$ via the following formula:

$$R^n_{\theta_{\max}}(f) = R^i(f) + \frac{k_\rho - k^i_\rho}{k^{i+1}_\rho - k^i_\rho} \cdot R^{i+1}(f), \quad i = 0, 1, \ldots, n-2 \tag{12}$$

where,

$$k_\rho = \frac{2\pi f \sin\theta_{\max}}{C_0}, k^i_\rho \leq k_\rho \leq k^{i+1}_\rho \tag{13}$$

2) Calculate $k^{i'}_\rho = \frac{(k_\rho)_{\max}}{2n} \cdot i', i' = 1, 3, \ldots, 2n-1$. For each $k^{i'}_\rho$, run the simulation to obtain $R^{i'}(f)$. Then compute $R^{2n}_{\theta_{\max}}(f)$ and ϵ according to (11)–(12).

3) If ϵ is within the tolerance, stop; else, set $n = 2n$, and go back to step 2).

The initial value of n can be an arbitrary even value. In this paper, $n = 12$ is adopted. Using this method, the same number of sampling points needs to be calculated at each step. As a result, much computational cost can be saved. Further more, this method is very suitable for parallel computation by assigning the jobs according to horizontal wave-number sample points.

Let us take the structure in Figure 2 as an example to illustrate the method. The dimensions in the figure are: $a = 5.6$ mm, $b = 5$ mm, $c = d = 0.3$ mm, the relative permittivity of the substrate is 4.8, and the height is 3.6 mm. The maximum incident angle is $\theta_{\max} = 60°$. The original number of sampling points is chosen as 12. The transmission coefficient simulated with FDTD over 6.5 GHz$\sim$13.5 GHz is shown in Figure 3. The relative error ϵ satisfies the accuracy requirement $\epsilon < 0.05$ after two iterations (24 sampling points were calculated).

3. NUMERICAL EXAMPLES

In this section, two periodic structures are simulated to validate the accuracy of the direct spectral FDTD method (DSFDTD). The first structure is the split-ring resonator (SRR) shown in Figure 2. The dimensions are given in Section 2.2. Since the periodic length is small relative to the resonance wavelength, only the dominant mode works. Here the frequency-domain solver of CST Microwave Studio (CST MWS) 2009 is chosen to compute the transmission coefficients of TE_{00} and TM_{00} modes. The calculated transmission coefficients for $\theta = 40°$ both in TE^z and TM^z are shown in Figures 4(a) and (b). The computed results by the direct spectral FDTD method are compared with those calculated by CST MWS for $\varphi = 30°$ and $\varphi = 60°$. It can be seen that those results agree very well.

The second structure is a dielectric grating slab shown in Figure 5(a). The structure is not very simple to be studied because its spectral responses exhibit some singularities that are very hard

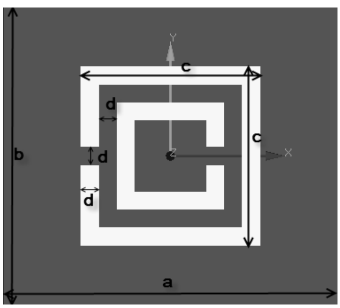

Figure 2. The sketch for the single split ring resonator (SRR) structure.

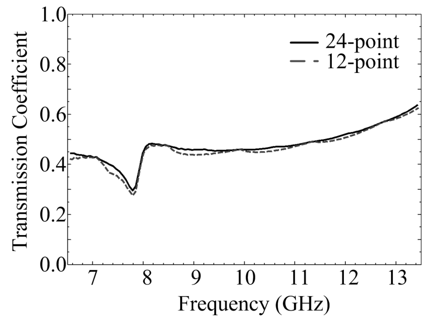

Figure 3. The transmission coefficient over 6.5 GHz∼13.5 GHz at $\theta = 60°$, $\varphi = 60°$.

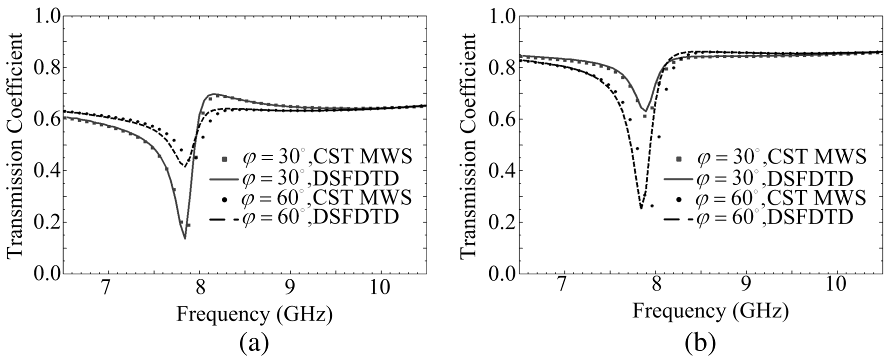

Figure 4. The transmission coefficients of SRR (a) $\theta = 40°$, TE^z; (b) $\theta = 40°$, TM^z.

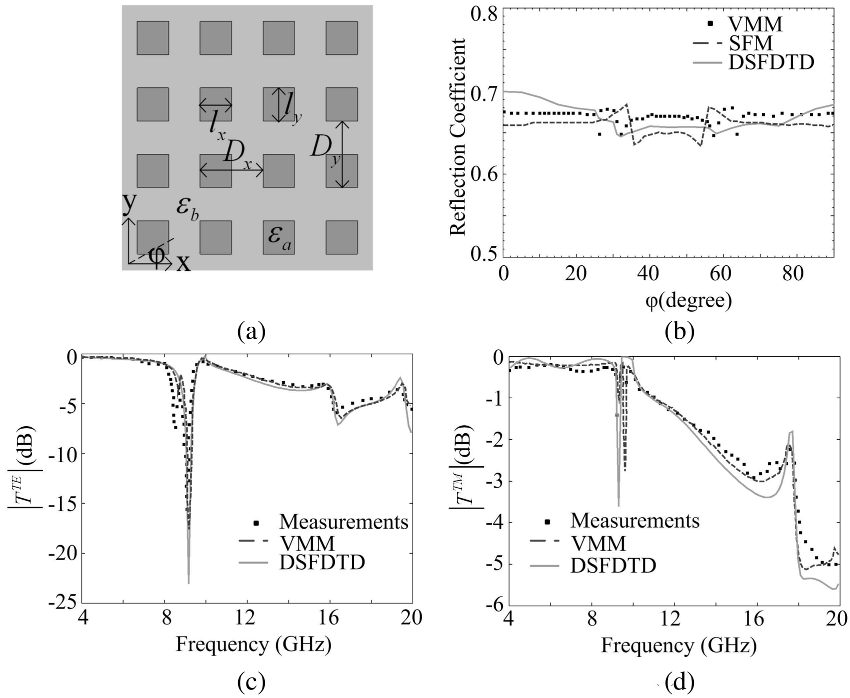

Figure 5. (a) the sketch of the slab-grating; (b) TE^z reflection coefficients of a two-dimensional grating with $\varepsilon_b = 4$, $\varepsilon_a = 10$, $l_x = l_y = 10\,\mathrm{mm}$, $D_x = D_y = 20\,\mathrm{mm}$, $h = 2\,\mathrm{mm}$, $\theta = 30°$ and $f = 10\,\mathrm{GHz}$; (c) and (d) TE^z and TM^z transmission coefficients of a one-dimensional grating with $\varepsilon_b = 1$, $\varepsilon_a = 2.59$, $\tan\delta = 0.0067$, $l_x = 30\,\mathrm{mm}$, $l_y = 15\,\mathrm{mm}$, $D_x = D_y = 30\,\mathrm{mm}$, $h = 8.7\,\mathrm{mm}$, $\varphi = 90°$ and $\theta = 1°$.

to handle by a theoretical or a numerical method [5]. Firstly, a one-dimensional dielectric grating slab with $\varepsilon_b = 1$, $\varepsilon_a = 2.59$, and $D_x = D_y = 30\,\mathrm{mm}$ is analyzed. The dimension of the dielectric rod is $30\,\mathrm{mm}\times 15\,\mathrm{mm}$. The loss tangent of the rods is $\tan\delta = 0.0067$. The thickness of the substrate is $h = 8.7\,\mathrm{mm}$. The direction of the incident plane wave is $\varphi = 90°$ and $\theta = 1°$. The transmission coefficients of the dielectric grating for both TE^z and TM^z incident waves are calculated. The vectorial modal method (VMM) is a semi-analytical technique which has been used to model two-dimensional (2D) dielectric grating and magneto-dielectric grating slab [15, 16]. We compare our results for the one-dimensional dielectric grating slab with the calculated

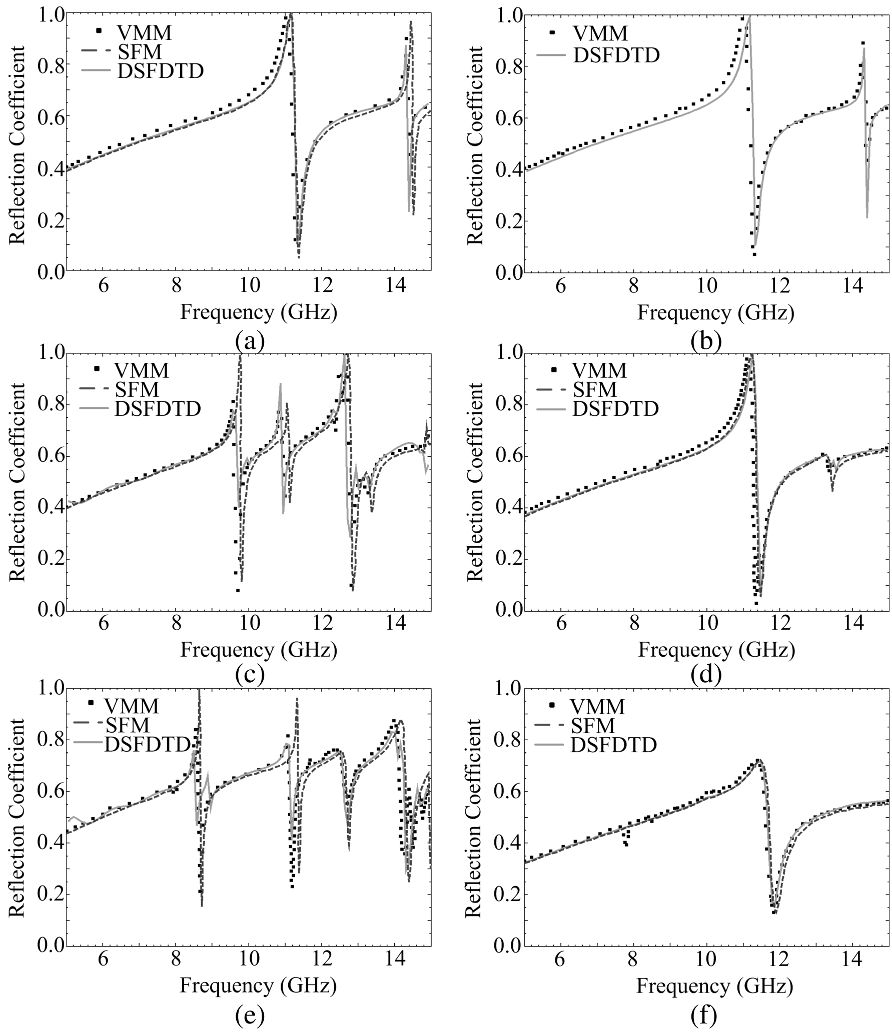

Figure 6. The reflection coefficients of a two-dimensional grating with $\varepsilon_b = 4$, $\varepsilon_a = 10$, $l_x = l_y = 10\,\text{mm}$, $D_x = D_y = 20\,\text{mm}$, $h = 2\,\text{mm}$ and $\varphi = 0°$. (a) $\theta = 0°$, TE^z; (b) $\theta = 0°$, TM^z; (c) $\theta = 15°$, TE^z; (d) $\theta = 15°$, TM^z; (e) $\theta = 30°$, TE^z; (f) $\theta = 30°$, TM^z.

results with the vectorial modal method and the experiment results of Tibuleac et al. [17]. These results are presented in Figures 5(c) and (d) and show good agreements. Next, a two-dimensional dielectric grating slab with $l_x = l_y = 10\,\text{mm}$, $D_x = D_y = 20\,\text{mm}$, $\varepsilon_a = 10$, $\varepsilon_b = 4$ is calculated. The thickness of the substrate is 2 mm. Figure 5(b) shows the reflection coefficients of the grating slab in TM^z polarization for $\theta = 30°$ with respect to φ. The observed frequency is $f = 10\,\text{GHz}$. We compare our results with the vectorial modal method and the split-field method (SFM) [5]. Comparisons show small discrepancies. The calculation error can be related to the spatial discretization because the FDTD becomes accurate only if this spatial step tends to zero. It is excepted that the calculation error decreases when the spatial step becomes smaller. Then the φ angle is fixed to be zero degree and the calculated reflection coefficients for $\theta = 0°$, $\theta = 15°$, and $\theta = 30°$ both in TE^z and TM^z are shown in Figure 6. Comparisons between above two methods (VMM and SFM) and the direct spectral FDTD method are made except for $\theta = 0°$ and TM^z polarization. Once again, good agreements between these results are observed.

4. CONCLUSIONS

In this paper, the direct spectral FDTD method is extended to compute the scattering of periodic structures when plane waves are incident from an arbitrary angle where both the azimuth and the elevation angles vary. An adaptive method is proposed to determine the horizontal wave-number sampling points. Numerical results show that this method is robust and accurate.

ACKNOWLEDGMENT

This work was supported in part by the Natural Science Foundation of China (NSFC) under Grant No. 60921063 and 60802001 and in part by National 973 project 2010CB327400.

REFERENCES

1. Taflove, A. and S. C. Hagness, *Computational Electrodynamics: The Finite-Difference Time-Domain Method*, 3rd edition, Artech House, Norwood, 2005.
2. Veysoglu, M. E., R. T. Shin, and J. A. Kong, "A finite-difference time-domain analysis of wave scattering from periodic surfaces: Oblique incident case," *Journal of Electromagnetic Waves and Applications*, Vol. 7, No. 12, 1595–1607, 1993.
3. Kao, Y. C. A. and R. G. Atkins, "A finite difference-time domain approach for frequency selective surfaces at oblique incidence," *Proc. IEEE AP-S Int. Symp.*, Vol. 2, 1432–1435, 1996.

4. Roden, J. A., S. D. Gedney, M. P. Kesler, J. G. Maloney, and P. H. Harms, "Time-domain analysis of periodic structures at oblique incidence: Orthogonal and nonorthogonal FDTD implementations," *IEEE Trans. Microwave Theory Tech.*, Vol. 46, No. 4, 420–427, 1998.
5. Belkhir, A. and F. I. Baida, "Three-dimensional finite-difference time-domain algorithm for oblique incidence with adaptation of perfectly matched layers and nonuniform meshing: Application to the study of a radar dome," *Physical Review E.*, Vol. 77, No. 5, 056701, 2008.
6. Mohammad Amjadi, S. and M. Soleimani, "Design of band-pass waveguide filter using frequency selective surfaces loaded with surface mount capacitors based on split-field update FDTD method," *Progress In Electromagnetics Research B*, Vol. 3, 271–281, 2008.
7. Aminian, A. and Y. Rahmat-Samii, "Spectral FDTD: A novel computational technique for the analysis of periodic structures," *Proc. IEEE AP-S Int. Symp.*, Vol. 3, 3139–3142, 2004.
8. Zheng, G., A. A. Kishk, A. W. Glisson, and A. B. Yakovlev, "A novel implementation of modified Maxwell's equations in the periodic finite-difference time-domain method," *Progress In Electromagnetics Research*, Vol. 59, 85–100, 2006.
9. Zheng, G., A. A. Kishk, A. W. Glisson, and A. B. Yakovlev, "Implementation of mur's absorbing boundaries with periodic structures to speed up the design process using fiite-difference time-domain method," *Progress In Electromagnetics Research*, Vol. 58, 101–114, 2006.
10. Ren, J., O. P. Gandhi, L. R. Walker, J. Fraschilla, and C. R. Boerman, "Floquent-based FDTD analysis of two-dimensional phased array antennas," *IEEE Microwave and Guided Wave Lett.*, Vol. 4, No. 4, 109–111, 1994.
11. Harms, P., R. Mittra, and W. Ko, "Implementation of the periodic boundary condition in the finite-difference time-domain algorithm for FSS structures," *IEEE Trans. Antennas Propagat.*, Vol. 42, No. 9, 1317–1324, 1994.
12. Aminian, A., F. Yang, and Y. Rahmat-Samii, "Bandwidth determination for soft and hard ground planes by spectral FDTD: A unified approach in visible and surface wave regions," *IEEE Trans. Antennas Propagat.*, Vol. 53, No. 1, 18–28, 2005.
13. Yang, F., J. Chen, R. Qiang, and A. Elsherbeni, "A simple and efficient FDTD/PBC algorithm for periodic structure analysis," *Radio Science*, Vol. 42, No. 4, RS4004, 2007.

14. Yang, F., J. Chen, R. Qiang, and A. Elsherbeni, "FDTD analysis of periodic structures at arbitrary incidence angles: A simple and efficient implementation of the periodic boundary conditions," *Proc. IEEE AP-S Int. Symp.*, Vol. 3, 2715–2718, 2006.
15. Attiya, A. M. and A. A. Kishk, "Modal analysis of a two-dimensional dielectric grating slab excited by an obliquely incident plane wave," *Progress In Electromagnetics Research*, Vol. 60, 221–243, 2006.
16. Attiya, A. M., A. A. Kishk, and A. W. Glisson, "Analysis of two-dimensional magneto-dielectric grating slab," *Progress In Electromagnetics Research*, Vol. 74, 195–216, 2007.
17. Tibuleac, S., R. Magnusson, T. A. Maldonado, P. P. Young, and T. R. Holzheimer, "Dielectric frequency-selective structures incorporating waveguide gratings," *IEEE Trans. Microwave Theory Tech.*, Vol. 48, 553–561, 2000.